Turkish Journal of Electrical Engineering & Computer Sciences

http://journals.tubitak.gov.tr/elektrik/

Research Article

Turk J Elec Eng & Comp Sci
(2016) 24: 4693 – 4706

doi:10.3906/elk-1404-341

# Variation of photovoltaic system performance due to climatic and geographical conditions in Turkey

**Betül BEKTAŞ EKİCİ***
Department of Architecture, Faculty of Architecture, Fırat University, Elazığ, Turkey

**Received:** 15.04.2014 • **Accepted/Published Online:** 28.08.2015 • **Final Version:** 06.12.2016

**Abstract:** This study focuses on the effect of climatic and geographical factors on the performance of photovoltaic systems. For this purpose, 4 different cities (Antalya, İstanbul, Elazığ, and Erzurum) from different climatic zones according to TS 825 Thermal Insulation Requirements in Buildings were selected. The monthly average global and diffuse solar radiation of the cities was calculated numerically with the long-term sunshine duration data (between 1990 and 2012) taken from the Turkish State Meteorological Service. The yearly electric energy generated by the grid-connected photovoltaic systems assumed to be located on the flat roofs of building samples were calculated for each of the cities. PVsyst 6.2.6. software was employed for the calculation of yearly energy yield. Consequently, the maximum photovoltaic output was achieved in Elazığ and the minimum in İstanbul. The optimum tilt angles for Antalya, İstanbul, Elazığ, and Erzurum were obtained as 32°, 36°, 32°, and 35°, respectively.

**Key words:** Photovoltaics, PVsyst, flat roofs, optimum tilt angle

## 1. Introduction

As a developing country, Turkey meets its energy needs with nonrenewable (fossil) energy sources like natural gas, coal, and fuel oil. Hence, studies concerning energy generally include measures for the efficient use of these energy sources [1–6]. However, significant benefits can be achieved by replacing the use of fossil fuels, which are expensive, at risk of depletion, and cause pollution. While the search for solutions of the energy and ecological problems of the 2000s is still continuing, the sun is at the forefront of renewable sources.

Photovoltaics (PV), the technology that converts solar energy to electrical energy, has the potential to become very common in the near future. Developments in the technology that increases efficiency and reduces costs have given rise to the use of PV in water pumping, solar home systems, communication, satellites, large-scale power plants, etc. [7]. High power capacity per unit weight, silent operation, no need for an active cooling system, and easy installation are the main advantages of PV technology [8]. Building-integrated photovoltaics (BIPV) is one recent solution for buildings' electric energy requirements. The system can be installed on roofs (flat/slope), façades, and shading systems of buildings [9].

In the literature, Oluklulu [10] searched the usability of PV modules by investigating the development and production structure of the energy sector, both in Turkey and on a global scale. Çelebi [11] presented the possibilities of PV mounted vertical building envelopes in terms of basic design rules. Tian et al. [12]

*Correspondence: bbektas@firat.edu.tr

investigated the effect of urban climate on the performance of PV modules and evaluated the PV power output with 3 different models by comparing the results with PV modules in rural areas. Peng et al. [13] discussed problems of existing BIPV structures. They gave insight into preferences for building integrated or attached PVs. Finally, they suggested a PV building structure that provides for effective maintenance and replacement of the PV elements. Urbanetz et al. [14] compared the annual power generation of a curved BIPV on the rooftop of a carport with an ideally oriented and tilted BIPV system installed on a building's roof at 27° S latitude. They found that the curved BIPV produced 12% less energy than the latitude-tilted one. Yoo et al. [15] used BIPV as both a solar shading component and a power generation element. Thus, they achieved reduced cooling loads through a sunshade PV panel and found that the ideal tilt of the photovoltaic array in Gihung, Korea, may not be practical when aesthetics, cost, and safety are considered. Glassmire et al. [16] investigated the effects of PV on electricity consumption requirements and cost at a large-scale facility. Kateris et al. [17] presented a calculation model for forecasting solar-suitable roof areas in Greece. After analyzing 129 representative buildings with actual measurements, they validated the developed model with 80 building samples and showed that the model was efficient and provided reliable results. Ioannou et al. [18] developed a design methodology for the optimum configuration of photovoltaic rows installed on rooftops by considering the impact of solar and dimensional parameters on power generation. They supported their work with a case study. Masa-Bote and Caamon-Martin [19] improved a model for predicting the electricity production of BIPV systems, which takes shading losses into account. The validation of the method was done with real data taken from 2 similar PV systems placed on the southern façade of the Technical University of Madrid. Kulaksız [20] suggested an ANFIS model to estimate equivalent parameters of PV modules such as series resistance, shunt resistance, and diode ideality factor. Güney and Onat [21] designed an automatic voltage regulator fed by PV cells used to excite a synchronous generator. They also supported their system with a real-life system application by examining its steady-state performance.

Studies concerning PV technology in Turkey generally deal with local samples. The novelty of this study is in looking at the issue from a wider perspective and the examination of system performance variations due to climatic and geographical factors. The objective of this paper is to investigate the potential of different PV technologies and optimum tilt angles of PV plants due to the climatic and geographical conditions of Turkey. In Turkey, there are 81 provinces; it is hard to determine the optimum PV system potentials for all of these locations. In order to limit the application study, we chose representative locations. Although the cities (Antalya, İstanbul, Elazığ, and Erzurum) were selected randomly, 4 different climatic regions, as determined in TS 825 Thermal Insulation Requirements in Buildings [22], were taken into consideration. During the selection process, we attempted to select cities located at different latitudes and as far from each other as possible, which represented the characteristics of each climatic region. The monthly global and diffuse solar radiation for all of the cities was calculated numerically with a computer program written in MATLAB by using daily sunshine duration data for a 22-year period (between 1990 and 2012) taken from the Turkish State Meteorological Service. The electrical energy generation of the PV installations was calculated with PVsyst 6.2.6 software. Five different PV technologies were employed to evaluate the PV electrical energy output. The annual electric energy production of PV plants was identified for different tilt angles varying between 0° and 50° with 5° steps. For determining the exact values of the optimum tilt angles, the same procedure was used for the refined search among tilt angles between 25° and 45° with 1° steps.

## 2. Case study

As a case study, the possibilities of grid-connected PV systems located in 4 different cities in Turkey from different climatic and geographical areas are presented. Climate zones (according to TS 825 Thermal Insulation Requirements in Buildings) and certain data of the selected cities can be seen in Table 1. The PV systems whose energy outputs were calculated were assumed to have been installed on flat roofs of buildings. The available area for the PV installation was considered to be 500 $m^2$ for each of the samples. The simplified schema of the PV plants is presented in Figure 1.

**Table 1.** Climate zones and certain data for selected cities.

| Climate zone | City | Altitude (m) | Longitude (E) | Latitude (N) |
|---|---|---|---|---|
| 1st | Antalya | 43 | 30° 42′ | 36° 53′ |
| 2nd | İstanbul | 30 | 29° 05′ | 40° 58′ |
| 3rd | Elazığ | 1015 | 39° 14′ | 38° 42′ |
| 4th | Erzurum | 1893 | 41° 17′ | 39° 55′ |

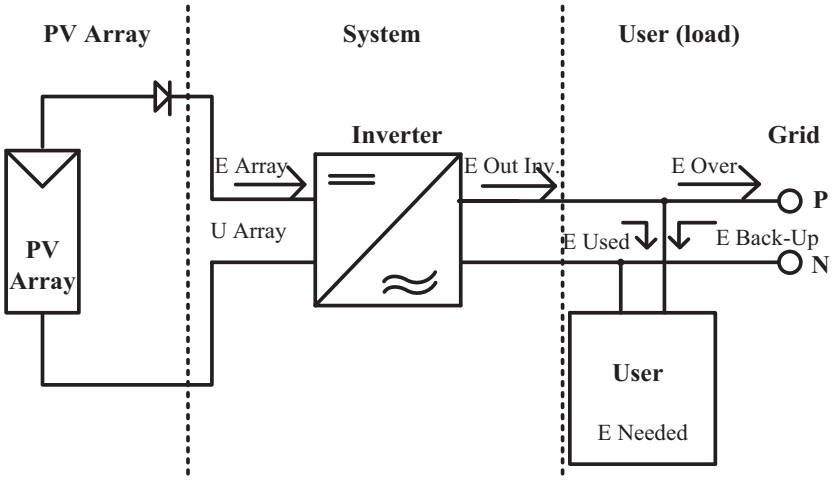


**Figure 1.** Simplified schema of the PV systems.

Engineers and architects need accurate solar radiation data for enhancing and sizing photovoltaics [23]. It is a vital factor that affects system performance. In this study, the hourly solar radiation of each location was calculated with the numerical method given in a previous study [24]. Daily sunshine duration data of the cities for a period of 22 years between 1990 and 2012 were taken from the Turkish State Meteorological Service. Solar radiation calculations were carried out with a computer program written in MATLAB R2012a software [25]. The monthly average values of global and diffuse radiation on horizontal surfaces of the selected cities are shown in Figures 2 and 3, respectively. The monthly average ambient temperatures of the representative cities are given in Table 2. Premodule losses such as dirt and snow were disregarded during the calculation period. The default values of premodule losses (0%) were employed for each of the city samples.

A wide variety of PV units produced with different technologies are available today. In this study, commercial modules of 5 different PV technologies on the market (monocrystalline silicon, si-mono; polycrystalline silicon, si-poly; copper indium diselenide, CIS; cadmium telluride, CdTe; and amorphous silicon, a-si) were considered.

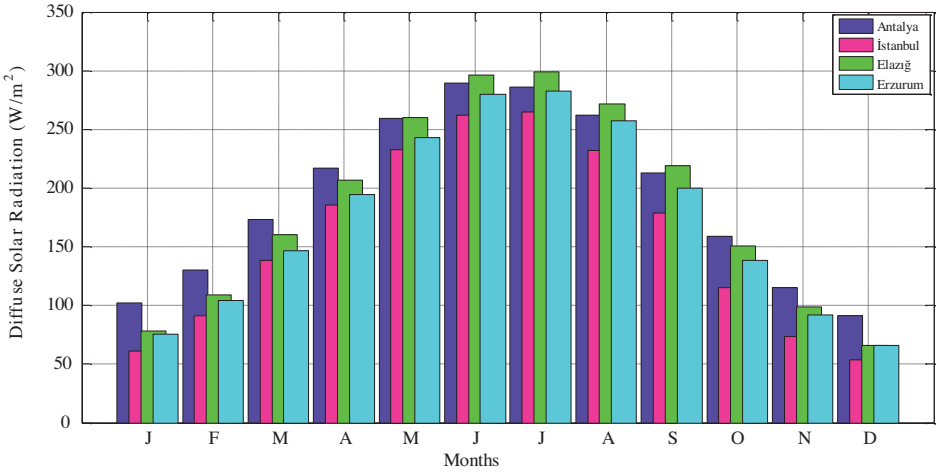


**Figure 2.** Monthly global solar radiation on horizontal surfaces in the selected cities.

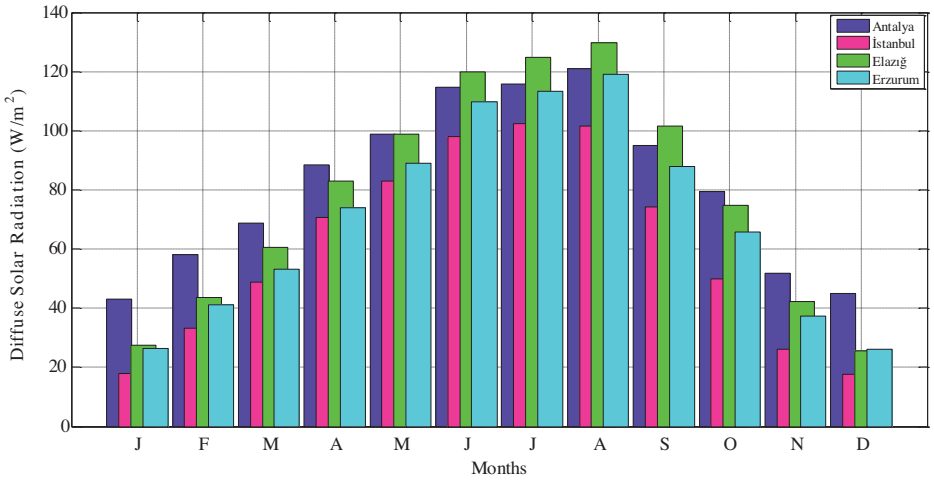


**Figure 3.** Monthly diffuse solar radiation on horizontal surfaces in the selected cities.

**Table 2.** Monthly average ambient temperatures (° C).

| Month | Cities | | | |
|---|---|---|---|---|
| | Antalya | İstanbul | Elazığ | Erzurum |
| January | 9.51 | 6.31 | –0.51 | –11.16 |
| February | 10.12 | 6.29 | 0.74 | –9.96 |
| March | 12.45 | 8.19 | 6.32 | –3.13 |
| April | 15.79 | 12.37 | 11.83 | 5.21 |
| May | 20.65 | 17.14 | 17.01 | 10.50 |
| June | 25.66 | 22.00 | 23.00 | 14.79 |
| July | 28.59 | 24.53 | 27.43 | 19.17 |
| August | 28.30 | 24.16 | 26.85 | 19.37 |
| September | 24.59 | 20.47 | 21.09 | 13.85 |
| October | 20.18 | 16.18 | 14.60 | 7.65 |
| November | 14.50 | 11.66 | 6.81 | –0.36 |
| December | 11.03 | 8.26 | 1.99 | –7.68 |

The technical details of the PV modules are given in Table 3. Siemens Sinvert PVM UL inverters were used in the simulations. The power output of the triphase 60-Hz inverter is 12 kW and it is capable of delivering over 98% peak efficiency. Minimum peak power voltage is 125 V and maximum peak power voltage is 450 V.

**Table 3.** PV modules considered in simulations.

| Technology | Si-mono | Si-poly | CIS | CdTe | a-Si |
|---|---|---|---|---|---|
| Manufacturer | Solara | Generic | Wurth Solar | First Solar | Uni-Solar |
| Model | SM400SP | Poly.110Wp 72 Cells | WSG 0036 E080 | FS-375 | PVL-124 |
| Power (Wp) | 100 | 110 | 80 | 75 | 124 |
| Efficiency (%) | 12.20 | 13.84 | 11.04 | 10.46 | 6.37 |
| Voc (V) | 21.4 | 43.40 | 44 | 60.30 | 42 |
| Isc (A) | 5.9 | 3.4 | 2.5 | 1.81 | 5.1 |
| Vmpp (V) | 17.80 | 34.80 | 35 | 47.60 | 30 |
| Impp (A) | 5.6 | 3.15 | 2.3 | 1.08 | 4.1 |
| $\gamma$ | 0.857 | 1.015 | 1.494 | 1.58 | 4.417 |
| $\mu_{ISC}$(mA/° C) | 3.3 | 1.7 | 1.3 | 0.7 | 5.1 |
| Length (mm) | 1087 | 1335 | 1205 | 1200 | 5007 |
| Width (mm) | 557 | 673 | 605 | 600 | 394 |
| Weight (kg) | 8 | 10.5 | 11 | 12 | 7 |
| Frame | Aluminum | Laminate | Aluminum | Laminate | Laminate |

## 3. PVsyst software

The yearly energy production of the installed PV systems was calculated with PVsyst 6.2.6 software [26]. It is based on a one-diode model and capable of performing simplified or detailed analysis. This program is an effective tool in sizing, simulating, and analyzing PV systems [27–29]. It was developed by the University of Geneva (Switzerland) and is regarded as a reference in the sector. Although Meteonorm software can generate meteorological data for locations and this file can be used in simulations, the meteorological data (monthly average global and diffuse solar radiation on horizontal surfaces, and monthly mean ambient temperature) used in this study were entered into the program manually. The program has a large database of PV modules, inverters, and batteries either available or out of circulation.

## 4. PVsyst calculation method

PVsyst uses Shockley's one-diode model in describing the operation of a PV module [29]. The model consists of a linear independent current source in parallel to a diode, a series ($R_s$), and a shunt resistance ($R_{sh}$), as shown in Figure 4.

The main expression for determining the general one-diode model is written as given below [27]:

$$I = I_{ph} - I_o \left[ e^{\left( \frac{qV + IR_s}{\gamma_k N_{cs} T} \right) - 1} \right] - \frac{V + IR_s}{R_{sh}}, \tag{1}$$

where I is the current supplied by the module (A), $I_o$ is the inverse saturation current, depending on the temperature (A), and $I_{ph}$ is the photocurrent (A) proportional to the irradiance G, with a correction as a function of $T_c$, the effective temperature of the cells (K). q is the charge of the electron ($=1.602 \times 10^{-19}$ C) and V is the voltage at the terminals of the module (V). $N_{cs}$, Gamma, and k are the number of cells in

series, the diode quality factor normally between 1 and 2, and Boltzmann's constant ($=1.381 \times 10^{-23}$ J/K), respectively.

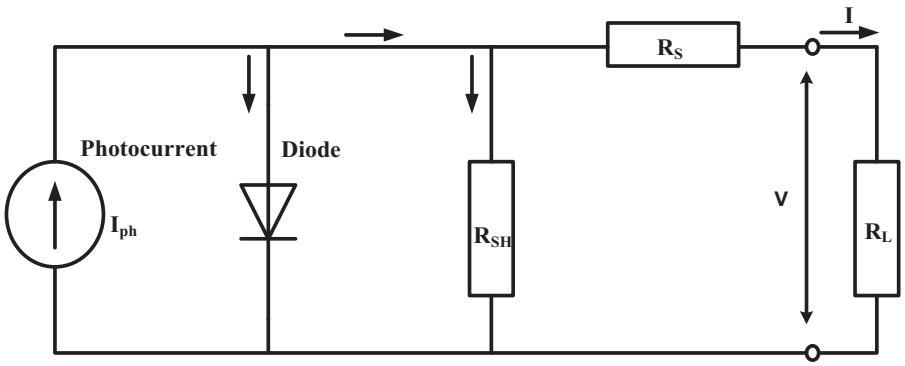


**Figure 4.** The equivalent circuit for explaining a PV cell.

The photocurrent varies proportionally with the effective irradiance level and the cell temperature. The model postulates that the photocurrent is proportional to the irradiation. Variation of photocurrent due to temperature is low. Thus, $I_{ph}$ is determined with the values given for reference conditions:

$$I_{ph} = \left(\frac{G}{G_{ref}}\right) \cdot [I_{phref} + mu_{ISC} \cdot (T_c - T_{cref})] \tag{2}$$

where G and $G_{ref}$ are effective and reference irradiances in W/m$^2$, respectively. $I_{phref}$ is the reference photocurrent in amperes. $T_{cref}$ is the reference cell's temperature (K). mu $_{ISC}$ is determined as the temperature coefficient of the short-circuit current.

The expression of the diode's reverse saturation related to the temperature is given in Eq. (3). $E_{gap}$ is the gap's energy of the material. In this study, it is employed as 1.12 eV for crystalline silicon, 1.03 eV for CIS, 1.5 eV for CdTe, and 1.7 eV for amorphous silicon.

$$I_o(T) = I_{oref} . \left(\frac{T_c}{T_{cref}}\right)^3 . \left[e^{\left(\frac{q.E_{gap}}{\gamma_k}\right).\left(\frac{1}{T_{cref}} - \frac{1}{T_c}\right)}\right] \tag{3}$$

The electrical performance of PV systems is strongly influenced by the thermal behavior of the field. This situation is defined by an energy balance between ambient temperature and cells heating up:

$$U.(T_c - T) = \alpha.G.(1 - \eta), \tag{4}$$

where $\alpha$ is the absorption coefficient of solar radiation and is assumed as 0.9 in this study. $\eta$ is the efficiency (%), and U is the thermal loss factor (W/m$^2$K). U is composed of a constant factor ($U_c$) and a factor proportional to the wind velocity ($U_v$), and expressed as follows. V in the equation is the wind velocity in m/s.

$$U = U_c + U_v.v \tag{5}$$

In this study, default values of the PVsyst software proposed for free-standing arrays, $U_c$ = 29 W/m$^2$K and $U_v$ = 0 W/m$^2$K/m/s, are used. As mentioned in Section 2, the monthly average global solar radiation data on horizontal surfaces were entered manually. The effective solar radiation on the tilted PV cell surface (G) is

the sum of beam, diffuse, and reflected components of the solar radiation. PVsyst uses Hay's model [30] for the calculation of the beam component and the Liu and Jordan model [31] for the diffuse components. The reflected component is calculated in relation to the albedo coefficient.

The fundamental formula for the calculation of the electrical energy generated by the PV plant ($E_{PV}$ (kWh)) is given in Eq. (5), where PR is the performance ratio (given in Eq. (7)) and $P_n$ is the nominal power of plant at standard test conditions (kW).

$$E_{PV} = PR.P_n.\frac{G}{G_{ref}}, \tag{6}$$

$$PR = k_\theta.k_Q.k_{\beta I}.k_\gamma.k_w.k_s.n_{inv}, \tag{7}$$

where $k_\theta$ is the optical reflection reduction factor, $k_Q$ is the quantum efficiency reduction factor, $k_{\beta I}$ is the low irradiance reduction factor, $k\gamma$ is the module temperature reduction factor, $k_w$ is the wiring losses reduction factor, $k_s$ is the soiling reduction factor, and $\eta_{inv}$ is the inverter conversion efficiency.

## 5. Results and discussion

The annual electrical energy generated by the grid-connected PV plants was calculated for 11 tilt angles from 0° to 50° with 5° steps. Five different PV technologies (si-mono, si-poly, CIS, CdTe, and a-Si) were employed separately. As seen from Figures 5–9, the maximum system outputs were obtained with tilt angles varying between 25° and 45° . For determining the exact optimum tilt angles for each of the locations, the annual system production data between 25° and 45° with 1° steps were calculated. In order to shorten the refined search process, only monocrystalline technology was considered, because the maximum solar radiation and maximum power output associated with this parameter are obtained by the optimum tilt angle. Hence, the optimum tilt angle is the same for all PV technologies. The results for the selected cities are shown in the charts given in Figure 10. In many studies [32,33], it has been claimed that the tilt angle should be equal to the local latitude for gathering the maximum output throughout the year. As can be seen from Figure 10, annual system production peaks at the 32° slope angle for Antalya and Elazığ, at 35° for Erzurum, and at 36° for İstanbul. All of the maximum power generations for the selected cities occurred at different tilt angles from the latitudes.

Although the installed capacities for the same installation area are different, the maximum annual energy yield is achieved with si-mono technology. This technology is approximately 32.5% more effective than si-poly technology according to the results of this study. The annual electric energy generated with this technology is greater than that of the PV plants using CIS, CdTe, and a-si technology at average rates of about 39%, 49.6%, and 149% respectively for all representative locations.

The maximum output of monocrystalline silicon-based PV plants for the cities located at different latitudes varies between 124.4 MWh and 108.1 MWh. Although Antalya is closer to the equator and therefore expected to obtain much more energy, the maximum energy yield was obtained at 38.4° N in Elazığ. As it is known that an increase in the PV module temperature has a negative effect on energy output, the high average ambient temperatures in the Antalya region decreased the system performance. If the monthly average ambient temperatures of Antalya and Elazığ were the same, the energy production would be more than 2.17% of the annual electricity production compared to the current situation. To see the effect of temperature on system performance, the electrical energy production of a monocrystalline PV plant installed in Antalya was calculated for different ambient temperature increases. For increases of 5, 10, 15, 20, and 25 ° C in ambient temperatures,

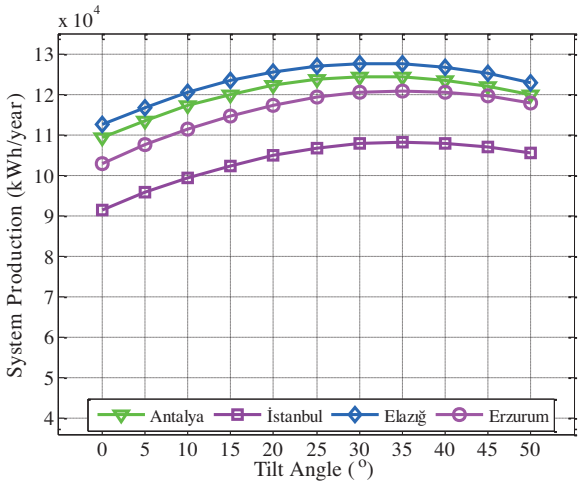


**Figure 5.** Annual system productions of PV installations (si-mono) for different tilt angles.

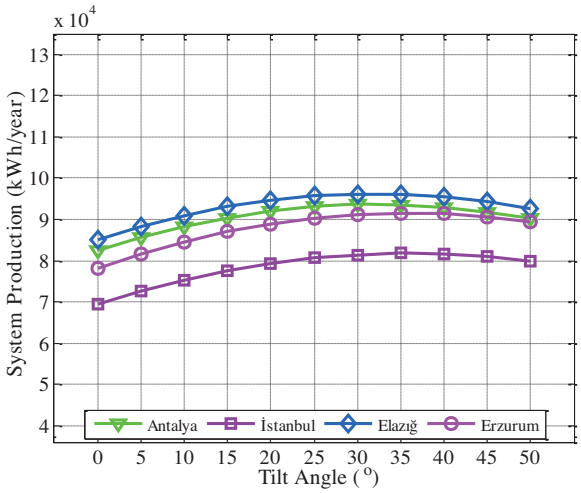


**Figure 6.** Annual system productions of PV installations (si-poly) for different tilt angles.

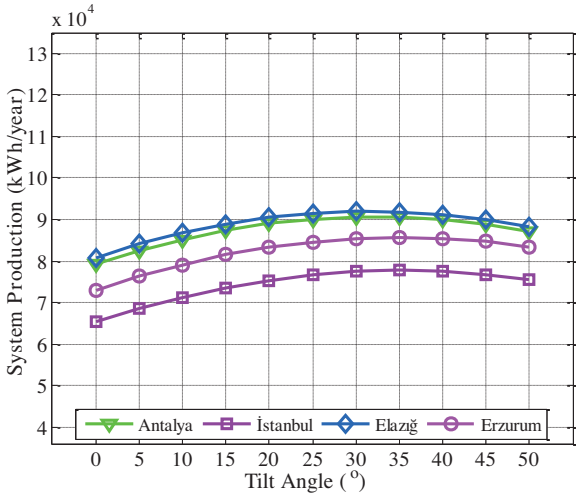


**Figure 7.** Annual system productions of PV installations (CIS) for different tilt angles.

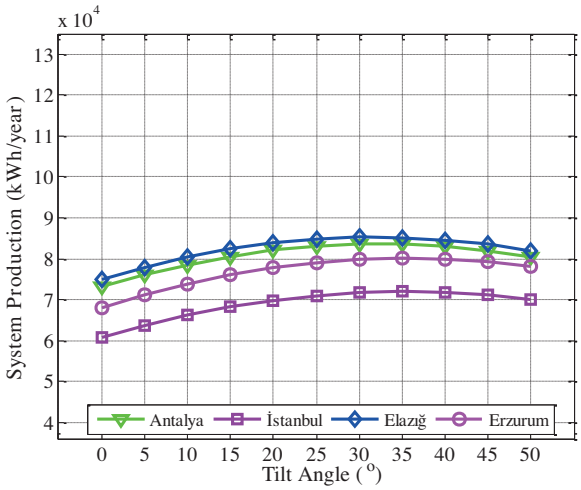


**Figure 8.** Annual system productions of PV installations (CdTe) for different tilt angles.

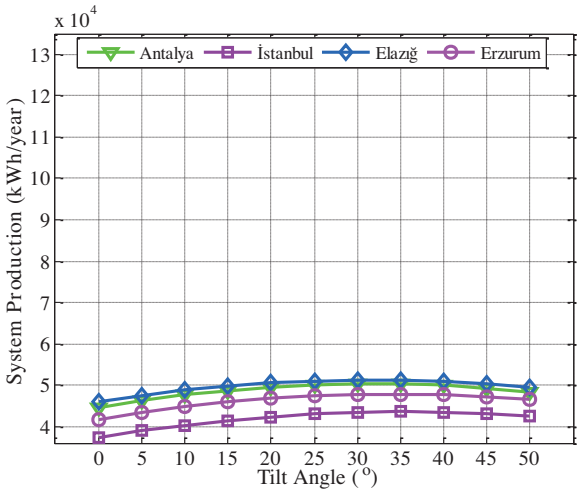


**Figure 9.** Annual system productions of PV installations (a-Si) for different tilt angles.

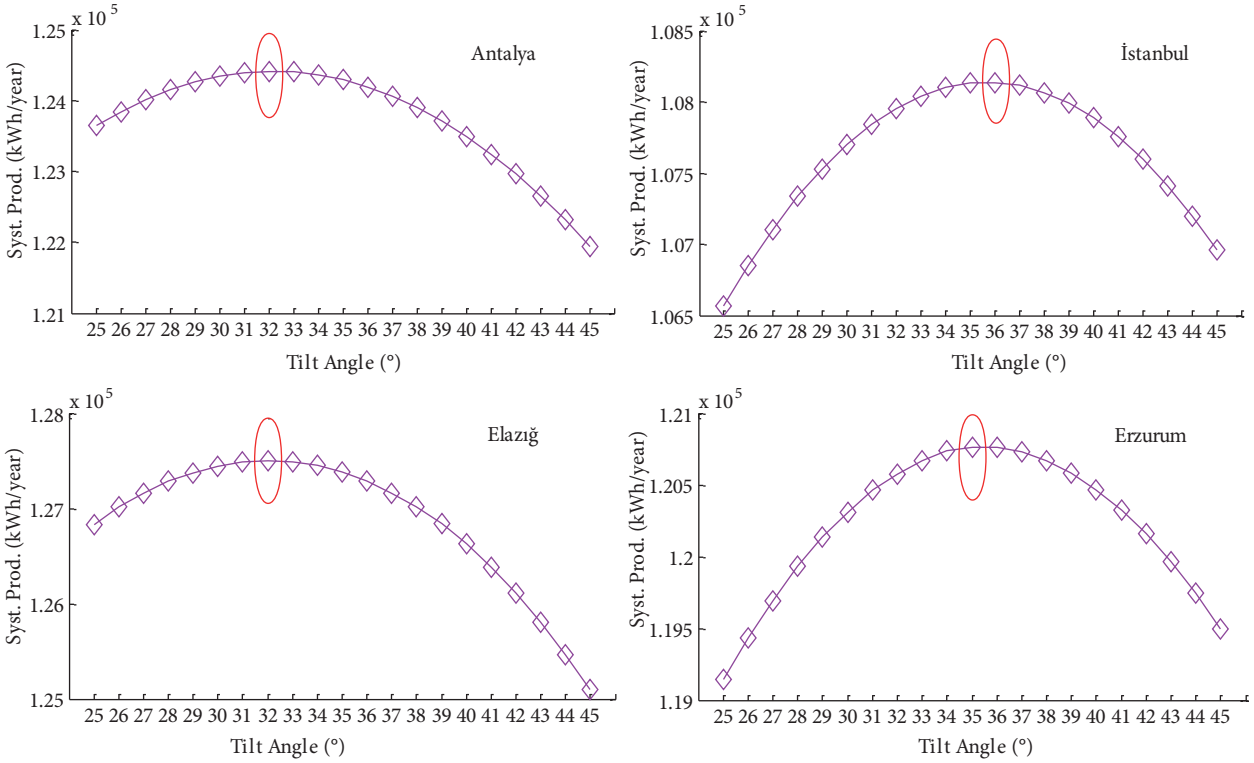


**Figure 10.** Optimum tilt angles for the representative cities.

the annual production was reduced by 2.5%, 4.6%, 6.9%, 9.2%, and 11.1%, respectively. The monthly system outputs depending on ambient temperature increases are shown in Figure 11.

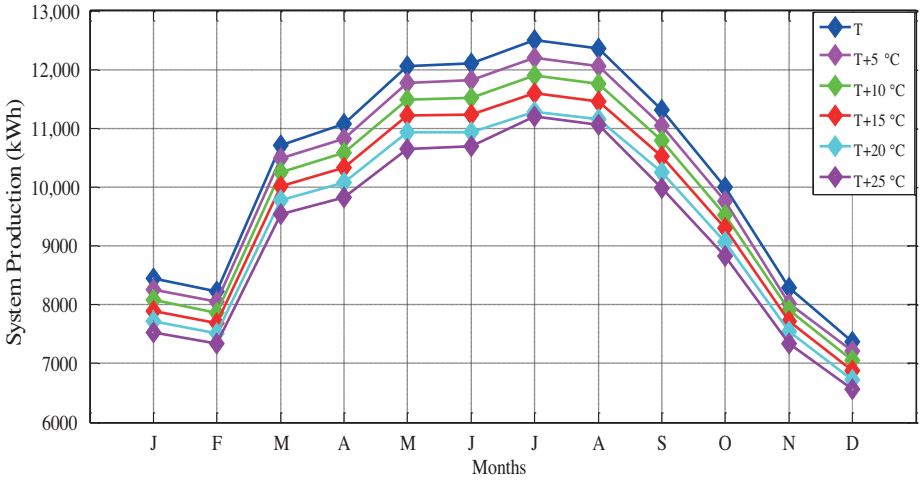


**Figure 11.** Energy production variation for different temperatures in Antalya.

For polycrystalline technology, the electrical energy generated in Antalya, Elazığ, and Erzurum was 93.16 MWh, 96.09 MWh, and 91.17 MWh, respectively. However, the peak power output in İstanbul was 81.43 MWh; this value is nearly 9.45% lower than those of the other cities.

When the results achieved with CdTe are evaluated, it is seen that the system production decreases to 83.5 MWh in Antalya, 71.7 MWh in İstanbul, 85.2 MWh in Elazığ, and 79.8 MWh in Erzurum. Among the different technology alternatives, the lowest electric output is obtained with amorphous silicon technology. The results are 59.84%, 46.82%, 44.19%, and 39.90% less than the outputs obtained from si-mono, si-poly, CIS, and CdTe PV plants, respectively. These values are nearly half of the yearly electricity production of the other PV technologies.

When the gradation of the cities in PV power generation are evaluated, it is seen that latitude is an important parameter in terms of solar radiation. However, in some special situations, climatic conditions such as ambient temperature (especially high temperatures) will have a greater effect, as seen in the case of Antalya. İstanbul is warmer than Erzurum throughout the year, but Erzurum is located at a lower latitude than İstanbul. Thus, the solar radiation intensity and the PV output energy in Erzurum are greater than those of İstanbul.

Specific production of the installation is an important indicator that shows the potential of the system by considering radiation conditions like orientation, location, and meteorological data. PV installations comprising different types of PV technologies have different installed powers due to the selected module dimensions and module powers. Hence, the nominal powers of each of the PV installations differ from each other. As the specific production is obtained by dividing the produced energy into the nominal power of the array, CIS technology provides the maximum specific production related to its proportionally low nominal power. The specific production rates of the PV installation samples for the selected cities are given in Table 4. It is seen from the table that the highest performance was also achieved with CIS technology as compared with the other alternatives.

**Table 4.** Specific productions of the PV installations for the selected cities.

| Location | Technology | Produced energy (MWh/year) | Total nominal power (kWp) | Specific yearly production (kWh/kWp) | Performance rate (%) |
|---|---|---|---|---|---|
| Antalya | Mono-silicon | 124.41 | 82.5 | 1508 | 79.3 |
| | Poly-silicon | 93.47 | 60.7 | 1539 | 80.9 |
| | CIS | 90.36 | 54.7 | 1651 | 86.8 |
| | CdTe | 83.21 | 52.0 | 1601 | 84.2 |
| | a-Si | 49.99 | 31.2 | 1600 | 84.1 |
| İstanbul | Mono-silicon | 108.14 | 82.5 | 1311 | 81.2 |
| | Poly-silicon | 81.57 | 60.7 | 1343 | 83.2 |
| | CIS | 77.37 | 54.7 | 1414 | 87.5 |
| | CdTe | 71.66 | 52.0 | 1379 | 85.4 |
| | a-Si | 42.99 | 31.2 | 1376 | 85.2 |
| Elazığ | Mono-silicon | 127.50 | 82.5 | 1545 | 80.7 |
| | Poly-silicon | 95.96 | 60.7 | 1580 | 82.5 |
| | CIS | 92.01 | 54.7 | 1681 | 87.8 |
| | CdTe | 85.26 | 52.0 | 1640 | 85.7 |
| | a-Si | 51.53 | 31.2 | 1649 | 86.1 |
| Erzurum | Mono-silicon | 120.76 | 82.5 | 1464 | 82.7 |
| | Poly-silicon | 91.53 | 60.7 | 1507 | 85.2 |
| | CIS | 85.99 | 54.7 | 1571 | 88.8 |
| | CdTe | 80.13 | 52.0 | 1542 | 87.1 |
| | a-Si | 48.41 | 31.2 | 1549 | 87.6 |

The performance ratio is a useful quality factor and independent from irradiation, and it does not represent the amount of produced energy. It quantifies the overall effect of premodule losses (shadows, dirt, snow, and

reflections), inverter losses, thermal losses, and conduction losses. These values can be improved by making some restorations in the system. When the performance rates determined for the optimum tilt angles for each of the city samples are ranked (Table 4), the lowest performance rates were obtained in Antalya and the highest in Erzurum. As all the system components are the same in all of the PV installations in each of the cities, this situation could only have been caused by temperature losses. Elazığ and İstanbul follow Antalya, respectively.

In order to evaluate the effect of altitude on PV energy generation, a numerical application was performed. As solar radiation is directly proportional to the energy output, the solar radiation on horizontal surfaces at different altitudes was calculated numerically. The sunshine duration and geographical location of İstanbul were employed for the determination of monthly average solar radiations at different altitudes varying between 0 m and 1000 m (Table 5). As shown in the table, a 500-m increase in altitude causes on average 2.8% and 1.5% more solar radiation in winter and in summer, respectively. A 1000-m increase causes 5.5% increase in winter and 3.1% in summer. The distance that the solar radiation has to pass through shortens, and the losses caused by this path therefore decrease. Thus, the PV installations at high altitudes are more productive than the ones located at low altitudes.

**Table 5.** The monthly average solar radiations related to different altitude values.

| Altitude | Months | | | | | | | | | | | |
|---|---|---|---|---|---|---|---|---|---|---|---|---|
| (m) | Jan | Feb | Mar | Apr | May | Jun | Jul | Aug | Sep | Oct | Nov | Dec |
| 0 | 60.8 | 91.2 | 138.4 | 185.7 | 232.6 | 262.2 | 264.9 | 231.7 | 178.5 | 115.4 | 73.1 | 53.9 |
| 100 | 61.1 | 91.7 | 138.9 | 186.3 | 23.4 | 262.9 | 265.8 | 232.4 | 179.1 | 115.8 | 73.5 | 54.2 |
| 200 | 61.4 | 92.1 | 139.5 | 187.0 | 234.2 | 263.8 | 266.6 | 233.1 | 179.7 | 116.3 | 73.8 | 54.5 |
| 300 | 61.8 | 92.5 | 140.1 | 187.7 | 234.9 | 264.6 | 267.4 | 233.9 | 180.3 | 116.7 | 74.1 | 54.8 |
| 400 | 62.1 | 92.9 | 140.6 | 188.4 | 235.8 | 265.4 | 268.2 | 234.6 | 180.8 | 117.2 | 74.5 | 55.1 |
| 500 | 62.4 | 93.3 | 141.2 | 189.1 | 236.6 | 266.3 | 268.9 | 235.3 | 181.4 | 117.6 | 74.8 | 55.4 |
| 600 | 62.7 | 93.7 | 141.7 | 189.8 | 237.3 | 267.1 | 269.8 | 235.9 | 182.0 | 118.1 | 75.2 | 55.7 |
| 700 | 63.1 | 94.1 | 142.3 | 190.5 | 238.1 | 267.9 | 270.6 | 236.7 | 182.6 | 118.5 | 75.5 | 55.9 |
| 800 | 63.4 | 94.6 | 142.8 | 191.2 | 238.9 | 268.7 | 271.4 | 237.4 | 183.2 | 118.9 | 75.9 | 56.3 |
| 900 | 63.7 | 94.9 | 143.4 | 191.9 | 239.7 | 269.6 | 272.2 | 238.1 | 183.8 | 119.4 | 76.2 | 56.6 |
| 1000 | 64.1 | 95.4 | 143.9 | 192.5 | 240.5 | 270.4 | 272.9 | 238.9 | 184.4 | 119.8 | 76.5 | 56.9 |

There are many manufacturers from Europe, Japan, India, and China in the market. This situation makes it difficult to make assessments about the costs. The unit prices of PV technologies decrease day by day in relation to reductions in processing cost and improvements in conversion coefficients. Figure 12 shows a downward trend in the cost of photovoltaic technologies. Nowadays, it is known that the unit prices of each of the mentioned technologies are under $1. The cost for the thin-film is no longer available as the market is commercially sensitive. These data can be derived from market studies that are generally provided by different organizations. Prices from September 2013 can be seen in Table 6. During the design stage, while choosing the appropriate PV technology, costs must be considered both with the available area for the installation and the required nominal power of the PV system.

## 6. Conclusion

In this paper, the behavior of grid-connected PV systems in different climatic zones and geographical sites of Turkey are investigated. The annual energy yield of 5 different PV technologies (si-mono, si-poly, CIS, CdTe, and a-si) were calculated for the same locations, and their performances were compared for different tilt angles.

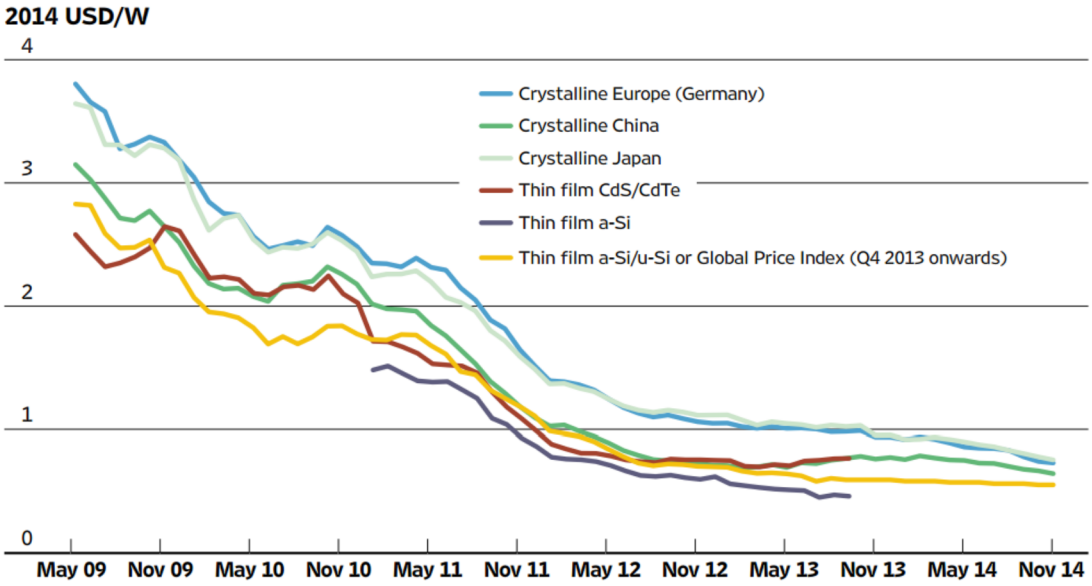


**Figure 12.** Average solar PV module prices by technology and manufacturing country [34].

**Table 6.** Unit prices of different types and origins of PV technologies [34].

| Type/origin | $/W |
|---|---|
| Crystalline | |
| Germany | 0.74 |
| China | 0.62 |
| Japan | 0.83 |
| Thin film | $/W |
| CdS/CdTe | 0.62 |
| a-Si | 0.38 |
| a-Si/$\mu$-Si | 0.48 |

The geographical position of the location (latitude) is an important indicator for PV power output. However, in some cases, the climatic conditions (especially ambient temperature) will be fundamental in performance determination. Maximum energy output was achieved in Elazığ (38.4° N), and the minimum energy output was produced in İstanbul (40.58° N). The maximum power generation was achieved with si-mono technology for each of the selected cities. It was determined that an increase in elevation leads to obtaining much more solar radiation and PV electric energy production.

The annual tilt angles of the modules are determined as 32° for Antalya and Elazığ, 35° for Erzurum, and 36° for İstanbul. However, adjusting the slope of the modules monthly or seasonally (for summer and winter conditions) due to the position of the sun would be more effective.

## References

[1] Diakaki C, Grigoroudis E, Kabelis N, Kolokotsa D, Kalaitzakis K, Stavrakakis G. A multi-objective decision model for improvement of energy efficiency in buildings. Energy 2010; 35: 5483-5496.

[2] Chung W, Hui YV, Lam YM. Benchmarking the energy efficiency of commercial buildings. Appl Energ 2006; 83: 1-14.

[3] Jain RK, Taylor JE, Perchiera G. Assessing eco-feedback interface usage and design to drive energy efficiency in buildings. Energ Buildings 2012; 48: 8-17.

[4] Kneifel J. Life-cycle carbon and cost analysis of energy efficiency measures in new commercial buildings. Energ Buildings 2010; 42: 333-340.

[5] Fischer C. Feedback on household electricity consumption: a tool for saving energy? Energy Efficiency 2008; 1: 79-104.

[6] Balaras CA, Drıutsa K, Argiriou AA, Asimakopoulos DN. Potential for energy conservation in apartment buildings. Energ Buildings 2000; 31: 143-154.

[7] Parida B, Iniyan S, Goic R. A review of solar photovoltaic technologies. Renew Sust Energ Rev 2011; 15: 1625-1636.

[8] Patel MR. Wind and Solar Power Systems: Design, Analysis, and Operation. 2nd ed. Boca Raton, FL, USA: Taylor & Francis, 2006.

[9] Bayod-Rujula A, Ortego-Bielsa A, Martinez-Gracia A. Photovoltaics on flat roofs. Energy 2011; 36: 1996-2010.

[10] Oluklulu Ç. A research on the photovoltaic modules that are being used actively in utilizing solar energy, sizing of the modules, and architectural using means of the modules. MSc, Gazi University, Ankara, Turkey, 2001 (in Turkish with English summary).

[11] Çelebi G. Using principles of photovoltaic panels on vertical building envelope. Gazi University Journal of Faculty of Engineering and Architecture 2002; 17: 17-33 (in Turkish with English abstract).

[12] Tian W, Wang Y, Ren J, Zhu L. Effect of urban climate on building integrated photovoltaics performance. Energy Conversion and Management 2007; 48: 1-8.

[13] Peng C, Huang Y, Wu Z. Building integrated photovoltaics (BIPV) in architectural design in China. Energ Buildings 2011; 43: 3592-3598.

[14] Urbanetz J, Debiazi Zomer C, Rüther R. Compromises between form and junction in grid connected building integrated photovoltaics (BIPV) at low latitude sites. Build Environ 2011; 46: 2107-2113.

[15] Yoo SH, Lee ET, Lee JK. Building integrated photovoltaics: a Korean case study. Sol Energy 1998; 64: 151-161.

[16] Glassmire J, Komor P, Lilienthal P. Electricity demand saving from distributed solar photovoltaics. Energ Policy 2012; 51: 323-331.

[17] Kateris M, Slini T, Papadopoulos AM. Urban energy potential in Greece: a statistical calculation model of suitable built roof areas for photovoltaics. Energ Buildings 2013; 62: 459-468.

[18] Ioannou AK, Stefanakis NE, Boudouvis AG. Design optimization of residential grid-connected photovoltaics on rooftops. Energ Buildings 2014; 76: 588-596.

[19] Masa-Bote D, Caamano-Martin E. Methodology for estimating building integrated photovoltaics electricity production under shadowing conditions and case study. Renew Sust Energ Rev 2014; 31: 492-500.

[20] Kulaksız AA. ANFIS-based estimation of PV module equivalent parameters: application to a stand-alone PV system with MPPT controller. Turk J Electr Eng Co 2013; 21: 2127-2140.

[21] Güney KRI, Onat N. Experimental analysis of an alternator excites with photovoltaic cells for small power plants. Turk J Electr Eng Co 2011; 19: 349-361.

[22] Turkish Standards Institute. TS 825. Thermal Insulation Requirements in Buildings. Ankara, Turkey: Turkish Standards Institution, 2008.

[23] Notton G, Cristofari C, Poggi P. Performance evaluation of various hourly slope irradiation models using Mediterranean experimental data of Ajaccio. Energ Convers Manage 2006; 47: 147-173.

[24] Aksoy UT, Bektaş Ekici B. Evaluation of the appropriateness of the climatic data of TS 825 for different degree-day regions. METU Journal of the Faculty of Architecture 2013: 30: 163-179.

[25] MathWorks. MATLAB Version R2012a. Natick, MA, USA: The MathWorks Inc., 2012.

[26] CUEPE. PVsyst, Version 6.26. Geneva, Switzerland: CUEPE, University of Geneva, 2014.

[27] Laudani A, Fulginei FR, Salvini A. Identification of the one-diode model for photovoltaic modules from datasheet values. Sol Energy 2014; 108: 432-446.

[28] Paoli C, Voyant C, Muselli M, Nivet ML. Forecasting of preprocessed daily solar radiation time series using neural networks. Sol Energy 2010; 84: 2146-2160.

[29] Aste N, Del Pero C, Leonforte F, Manfren M. A simplified model for the estimation of energy production of PV systems. Energy 2013; 59: 503-512.

[30] Hay JE. Calculation of monthly mean solar radiation for horizontal and inclined surfaces. Sol Energy 1979; 23: 301-307.

[31] Liu BHY, Jordan RC. Daily insolation on surfaces tilted towards the equator. Transactions of the ASHRAE 1962; 3: 526-541.

[32] Pavlovic T, Pavlovic Z, Pantic L, Kostic LJ. Determining optimum tilt angles and orientations of photovoltaic panels in Nis, Serbia. Contemporary Materials 2010; I: 151-156.

[33] Fletcher G. The Electrician's Guide to Photovoltaic System Installation. Clifton Park, NY, USA: Delmar, 2014.

[34] IRENA. Renewable Power Generation Costs. Berlin, Germany: IRENA Publications, 2014.